



**Autonomous Vehicle Simulation (AVS) Laboratory,
University of Colorado**

Basilisk Technical Memorandum

HINGEDRIGIDBODYSTATEEFFECTOR

Rev	Change Description	By	Date
1.0	Initial Draft	C. Allard	20170703
1.1	Format Changes	C. Allard	20170712
2.0	3 Additional Tests Added	C. Allard	20170728
2.1	Frequency and mag tests updated	C. Allard	20170803
2.2	Added hinge motor	H. Schaub	2020-09-22
2.3	Added config log output message	H. Schaub	2020-09-29

Contents

1	Model Description	1
1.1	Introduction	1
1.2	Equations of Motion	1
1.3	Back Substitution Method	2
1.4	Panel State Configuration Log Message Information	3
2	Model Functions	4
3	Model Assumptions and Limitations	4
4	Test Description and Success Criteria	4
4.1	Gravity and no damping scenario	5
4.2	No gravity and no damping scenario	5
4.3	No gravity with damping scenario	5
4.4	Steady State Deflection Verification Scenario	5
4.5	Frequency and Amplitude Verification Scenario	7
4.5.1	Frequency Test Description	7
4.5.2	Max Deflection While Force is Being Applied	8
4.5.3	Max Deflection While Force is Not Being Applied	8
4.6	Lagrangian vs Basilisk Scenario	9
5	Test Parameters	9
6	Test Results	11
6.1	Gravity with no damping scenario	11
6.2	No Gravity with no damping scenario	14
6.3	No Gravity with damping scenario	18
6.4	Steady State Deflection Scenario	21
6.5	Frequency and Amplitude Verification Scenario	23
6.6	Lagrangian vs Basilisk Scenario	23

1 Model Description

1.1 Introduction

The hinged rigid body class is an instantiation of the state effector abstract class. The state effector abstract class is a base class for modules that have dynamic states or degrees of freedom with respect to the rigid body hub. Examples of these would be reaction wheels, variable speed control moment gyroscopes, fuel slosh particles, etc. Since the state effectors are attached to the hub, the state effectors are directly affecting the hub as well as the hub is back affecting the state effectors.

Specifically, a hinged rigid body state effector is a rigid body that has a diagonal inertia with respect to its \mathcal{S}_i frame as seen in Figure 1. It is attached to the hub through a hinge with a linear torsional spring and linear damping term. An optional motor torque command can be used to actuate the panel. The dynamics of this multi-body problem have been derived and can be seen in Reference 1. The derivation

is general for N number of panels attached to the hub but does not allow for multiple interconnected panels.

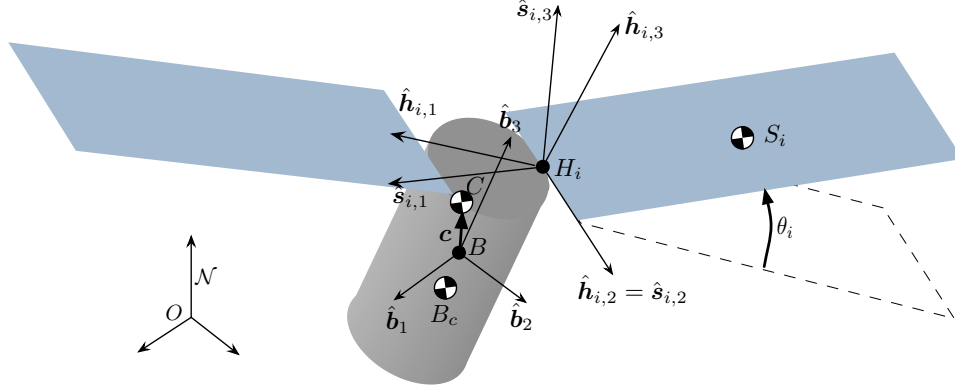


Fig. 1: Hinged rigid body frame and variable definitions

1.2 Equations of Motion

The following equations of motion (EOMs) are pulled from Reference 1 for convenience. Equation (1) is the spacecraft translational EOM, Equation (2) is the spacecraft rotational EOM, and Equation (3) is the hinged rigid body rotational EOM. These are the coupled nonlinear EOMs that need to be integrated in the simulation.

$$m_{sc}\ddot{\mathbf{r}}_{B/N} - m_{sc}[\tilde{\mathbf{c}}]\dot{\boldsymbol{\omega}}_{B/N} + \sum_i^N m_{sp_i} d_i \hat{\mathbf{s}}_{i,3} \ddot{\theta}_i = \mathbf{F}_{ext} - 2m_{sc}[\tilde{\boldsymbol{\omega}}_{B/N}]\mathbf{c}' - m_{sc}[\tilde{\boldsymbol{\omega}}_{B/N}][\tilde{\boldsymbol{\omega}}_{B/N}]\mathbf{c} - \sum_i^N m_{sp_i} d_i \dot{\theta}_i^2 \hat{\mathbf{s}}_{i,1} \quad (1)$$

$$m_{sc}[\tilde{\mathbf{c}}]\ddot{\mathbf{r}}_{B/N} + [I_{sc,B}]\dot{\boldsymbol{\omega}}_{B/N} + \sum_i^N \left\{ I_{s_i,2} \hat{\mathbf{h}}_{i,2} + m_{sp_i} d_i [\tilde{\mathbf{r}}_{S_i/B}] \hat{\mathbf{s}}_{i,3} \right\} \ddot{\theta}_i = - [\tilde{\boldsymbol{\omega}}_{B/N}][I_{sc,B}]\boldsymbol{\omega}_{B/N} - [I'_{sc,B}]\boldsymbol{\omega}_{B/N} - \sum_i^N \left\{ \dot{\theta}_i [\tilde{\boldsymbol{\omega}}_{B/N}] \left(I_{s_i,2} \hat{\mathbf{h}}_{i,2} + m_{sp_i} d_i [\tilde{\mathbf{r}}_{S_i/B}] \hat{\mathbf{s}}_{i,3} \right) + m_{sp_i} d_i \dot{\theta}_i^2 [\tilde{\mathbf{r}}_{S_i/B}] \hat{\mathbf{s}}_{i,1} \right\} + \mathbf{L}_B \quad (2)$$

$$m_{sp_i} d_i \hat{\mathbf{s}}_{i,3}^T \ddot{\mathbf{r}}_{B/N} + \left[(I_{s_i,2} + m_{sp_i} d_i^2) \hat{\mathbf{s}}_{i,2}^T - m_{sp_i} d_i \hat{\mathbf{s}}_{i,3}^T [\tilde{\mathbf{r}}_{H_i/B}] \right] \dot{\boldsymbol{\omega}}_{B/N} + (I_{s_i,2} + m_{sp_i} d_i^2) \ddot{\theta}_i = u_i - k_i \theta_i - c_i \dot{\theta}_i + \hat{\mathbf{s}}_{i,2}^T \boldsymbol{\tau}_{ext,H_i} + (I_{s_i,3} - I_{s_i,1} + m_{sp_i} d_i^2) \omega_{s_i,3} \omega_{s_i,1} - m_{sp_i} d_i \hat{\mathbf{s}}_{i,3}^T [\tilde{\boldsymbol{\omega}}_{B/N}][\tilde{\boldsymbol{\omega}}_{B/N}] \mathbf{r}_{H_i/B} \quad (3)$$

where u_i is the optional motor torque.

1.3 Back Substitution Method

In order to integrate the EOMs in a modular fashion, a back substitution method was developed and can be seen in Reference.¹ The hinged rigid body model must adhere to this analytical form, and the details are briefly summarized in the equations following. First the hinged rigid body EOM is substituted into the translational EOM and rearranged:

$$\begin{aligned} & \left(m_{sc}[I_{3 \times 3}] + \sum_{i=1}^N m_{sp_i} d_i \hat{\mathbf{s}}_{i,3} \mathbf{a}_{\theta_i}^T \right) \ddot{\mathbf{r}}_{B/N} + \left(-m_{sc}[\tilde{\mathbf{c}}] + \sum_{i=1}^N m_{sp_i} d_i \hat{\mathbf{s}}_{i,3} \mathbf{b}_{\theta_i}^T \right) \dot{\boldsymbol{\omega}}_{B/N} \\ & = m_{sc} \ddot{\mathbf{r}}_{C/N} - 2m_{sc}[\tilde{\boldsymbol{\omega}}_{B/N}] \mathbf{c}' - m_{sc}[\tilde{\boldsymbol{\omega}}_{B/N}][\tilde{\boldsymbol{\omega}}_{B/N}] \mathbf{c} - \sum_{i=1}^N \left(m_{sp_i} d_i \dot{\theta}_i^2 \hat{\mathbf{s}}_{i,1} + m_{sp_i} d_i c_{\theta_i} \hat{\mathbf{s}}_{i,3} \right) \end{aligned} \quad (4)$$

Following the same pattern for the hub rotational EOM, Eq. (2), yields:

$$\begin{aligned} & \left[m_{sc}[\tilde{\mathbf{c}}] + \sum_{i=1}^N (I_{s_{i,2}} \hat{\mathbf{s}}_{i,2} + m_{sp_i} d_i [\tilde{\mathbf{r}}_{S_{c,i}/B}] \hat{\mathbf{s}}_{i,3}) \mathbf{a}_{\theta_i}^T \right] \ddot{\mathbf{r}}_{B/N} \\ & + \left[[I_{sc,B}] + \sum_{i=1}^N (I_{s_{i,2}} \hat{\mathbf{s}}_{i,2} + m_{sp_i} d_i [\tilde{\mathbf{r}}_{S_{c,i}/B}] \hat{\mathbf{s}}_{i,3}) \mathbf{b}_{\theta_i}^T \right] \dot{\boldsymbol{\omega}}_{B/N} = -[\tilde{\boldsymbol{\omega}}_{B/N}][I_{sc,B}] \boldsymbol{\omega}_{B/N} - [I'_{sc,B}] \boldsymbol{\omega}_{B/N} \\ & - \sum_{i=1}^N \left\{ (\dot{\theta}_i [\tilde{\boldsymbol{\omega}}_{B/N}] + c_{\theta_i} [I_{3 \times 3}]) \left(I_{s_{i,2}} \hat{\mathbf{s}}_{i,2} + m_{sp_i} d_i [\tilde{\mathbf{r}}_{S_{c,i}/B}] \hat{\mathbf{s}}_{i,3} \right) + m_{sp_i} d_i \dot{\theta}_i^2 [\tilde{\mathbf{r}}_{S_{c,i}/B}] \hat{\mathbf{s}}_{i,1} \right\} + \mathbf{L}_B \end{aligned} \quad (5)$$

With the following definitions:

$$\mathbf{a}_{\theta_i} = -\frac{m_{sp_i} d_i}{(I_{s_{i,2}} + m_{sp_i} d_i^2)} \hat{\mathbf{s}}_{i,3} \quad (6a)$$

$$\mathbf{b}_{\theta_i} = -\frac{1}{(I_{s_{i,2}} + m_{sp_i} d_i^2)} \left[(I_{s_{i,2}} + m_{sp_i} d_i^2) \hat{\mathbf{s}}_{i,2} + m_{sp_i} d_i [\tilde{\mathbf{r}}_{H_i/B}] \hat{\mathbf{s}}_{i,3} \right] \quad (6b)$$

$$\begin{aligned} c_{\theta_i} = & \frac{1}{(I_{s_{i,2}} + m_{sp_i} d_i^2)} \left(u_i - k_i \theta_i - c_i \dot{\theta}_i + \hat{\mathbf{s}}_{i,2} \cdot \boldsymbol{\tau}_{\text{ext},H_i} + (I_{s_{i,3}} - I_{s_{i,1}} + m_{sp_i} d_i^2) \omega_{s_{i,3}} \omega_{s_{i,1}} \right. \\ & \left. - m_{sp_i} d_i \hat{\mathbf{s}}_{i,3}^T [\tilde{\boldsymbol{\omega}}_{B/N}] [\tilde{\boldsymbol{\omega}}_{B/N}] \mathbf{r}_{H_i/B} \right) \end{aligned} \quad (6c)$$

In Eq. (6c) the variable u_i is the motor torque acting on the i^{th} panel.

The equations can now be organized into the following matrix representation:

$$\begin{bmatrix} [A] & [B] \\ [C] & [D] \end{bmatrix} \begin{bmatrix} \ddot{\mathbf{r}}_{B/N} \\ \dot{\boldsymbol{\omega}}_{B/N} \end{bmatrix} = \begin{bmatrix} \mathbf{v}_{\text{trans}} \\ \mathbf{v}_{\text{rot}} \end{bmatrix} \quad (7)$$

Finally, the hinged rigid body model must make ‘‘contributions’’ to the matrices defined in Equations (7). These contributions are defined in the following equations:

$$[A_{\text{contr}}] = m_{\text{sp}_i} d_i \hat{\mathbf{s}}_{i,3} \mathbf{a}_{\theta_i}^T \quad (8)$$

$$[B_{\text{contr}}] = m_{\text{sp}_i} d_i \hat{\mathbf{s}}_{i,3} \mathbf{b}_{\theta_i}^T \quad (9)$$

$$[C_{\text{contr}}] = (I_{s_{i,2}} \hat{\mathbf{s}}_{i,2} + m_{\text{sp}_i} d_i [\tilde{\mathbf{r}}_{S_{c,i}/B}] \hat{\mathbf{s}}_{i,3}) \mathbf{a}_{\theta_i}^T \quad (10)$$

$$[D_{\text{contr}}] = (I_{s_{i,2}} \hat{\mathbf{s}}_{i,2} + m_{\text{sp}_i} d_i [\tilde{\mathbf{r}}_{S_{c,i}/B}] \hat{\mathbf{s}}_{i,3}) \mathbf{b}_{\theta_i}^T \quad (11)$$

$$\mathbf{v}_{\text{trans,contr}} = - \left(m_{\text{sp}_i} d_i \dot{\theta}_i^2 \hat{\mathbf{s}}_{i,1} + m_{\text{sp}_i} d_i c_{\theta_i} \hat{\mathbf{s}}_{i,3} \right) \quad (12)$$

$$\mathbf{v}_{\text{rot,contr}} = - \left\{ (\dot{\theta}_i [\tilde{\boldsymbol{\omega}}_{B/N}] + c_{\theta_i} [I_{3 \times 3}]) (I_{s_{i,2}} \hat{\mathbf{s}}_{i,2} + m_{\text{sp}_i} d_i [\tilde{\mathbf{r}}_{S_{c,i}/B}] \hat{\mathbf{s}}_{i,3}) + m_{\text{sp}_i} d_i \dot{\theta}_i^2 [\tilde{\mathbf{r}}_{S_{c,i}/B}] \hat{\mathbf{s}}_{i,1} \right\} \quad (13)$$

The final equation that is needed is:

$$\ddot{\theta}_i = \mathbf{a}_{\theta_i}^T \ddot{\mathbf{r}}_{B/N} + \mathbf{b}_{\theta_i}^T \dot{\boldsymbol{\omega}}_{B/N} + c_{\theta_i} \quad (14)$$

1.4 Panel State Configuration Log Message Information

The panel provides an output message `hingedRigidBodyConfigLogOutMsg` of type `SCStatesMsg`. This message contains the panel frame S_i position and attitude states. As this is a regular spacecraft state message, this output message can be piped to other modules such as the coarse sun sensor or solar panel power module spacecraft state input message. This allows the CSS or solar power evaluation to be performed relative to the time-varying panel configuration.

The configuration log records the following 4 message variables: `r_BN_N`, `r_BN_N`, `sigma_BN` and `omega_BN_B`. These states are evaluated using:

$$\mathbf{r}_{S_i/N} = \mathbf{r}_{S_i/B} + \mathbf{r}_{B/N} \quad (15)$$

$$\mathbf{v}_{S_i/N} = \dot{\mathbf{r}}_{B/N} + d_i \dot{\theta}_i \hat{\mathbf{s}}_{i,3} - d_i \boldsymbol{\omega}_{B/N} \times \hat{\mathbf{s}}_{i,1} + \boldsymbol{\omega}_{B/N} \times \mathbf{r}_{H_i/B} \quad (16)$$

$$\boldsymbol{\sigma}_{S_i/N} = \boldsymbol{\sigma}_{S_i/B} \otimes \boldsymbol{\sigma}_{B/N} \quad (17)$$

$$\boldsymbol{\omega}_{S_i/N} = \boldsymbol{\omega}_{B/N} + \dot{\theta}_i \hat{\mathbf{s}}_{i,2} \quad (18)$$

When storing these log state the message body frame is the hinge frame S_i .

2 Model Functions

This module is intended to be used an approximation to a flexing body attached to the spacecraft. Examples include solar arrays, antennas, and other appended bodies that would exhibit flexing behavior. Below is a list of functions that this model performs:

- Compute it's contributions to the mass properties of the spacecraft
- Provides matrix contributions for the back substitution method
- Compute it's derivatives for θ and $\dot{\theta}$
- Adds energy and momentum contributions to the spacecraft
- create an output message with the panel inertial position and attitude states

3 Model Assumptions and Limitations

Below is a summary of the assumptions/limitations:

- Is a first-order approximation to a flexing body
- Is developed in such a way that does not require constraints to be met
- The hinged rigid body must have a diagonal inertia tensor with respect the \mathcal{S}_i frame as seen in Figure 1
- Only linear spring and damping terms
- Will only approximate one flexing mode at a time
- Cannot simulate multiple interconnected panels
- The hinged rigid body will always stay attached to the hub (the hinge does not have torque limits)
- The hinge does not have travel limits, therefore if the spring is not stiff enough it will unrealistically travel through bounds such as running into the spacecraft hub
- The EOMs are nonlinear equations of motion, therefore there can be inaccuracies (and divergence) that result from integration. Having a time step of ≤ 0.10 sec is recommended, but this also depends on the natural frequency of the system
- When trying to match the frequency of a physical appended body, note that the natural frequency of the coupled system will be different than the appending body flexing by itself

4 Test Description and Success Criteria

This test is located in `simulation/dynamics/HingedRigidBodyStates/UnitTest/test_hingedRigidBodyStateEffector.py`. In this integrated test there are two hinged rigid bodies connected to the spacecraft hub. Depending on the scenario, there are different success criteria. These are outlined in the following subsections:

4.1 Gravity and no damping scenario

In this test the simulation is placed into orbit around Earth with point gravity and has no damping in the hinged rigid bodies. The following parameters are being tested.

- Conservation of orbital angular momentum
- Conservation of orbital energy
- Conservation of rotational angular momentum
- Conservation of rotational energy
- Achieving the expected final attitude

4.2 No gravity and no damping scenario

In this test, the spacecraft is placed in free space (no gravity) and has no damping in the hinged rigid bodies. The following parameters describe the success criteria.

- Conservation of orbital angular momentum
- Conservation of orbital energy
- Conservation of rotational angular momentum
- Conservation of rotational energy
- Achieving the expected final attitude (same final attitude as the Gravity with no damping scenario)
- Achieving the expected final position
- Conservation of velocity of center of mass

4.3 No gravity with damping scenario

In this test, the spacecraft is placed in free space (no gravity) and has damping in the hinged rigid bodies. The following parameters describe the success criteria.

- Conservation of orbital angular momentum
- Conservation of orbital energy
- Conservation of rotational angular momentum
- Conservation of velocity of center of mass

4.4 Steady State Deflection Verification Scenario

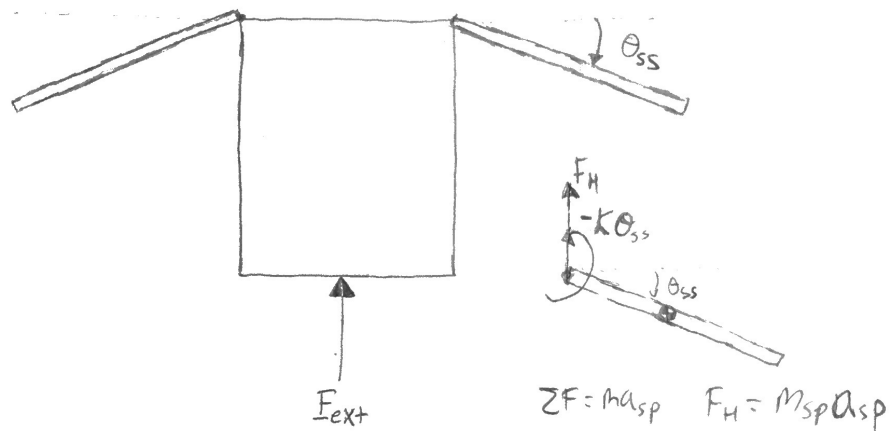
The BOE calculation for the steady state deflection can be seen in Fig. 2. The resulting steady state deflection does not have a closed form solution so a root solving function must be used to converge on the solution. A Newton-Raphson method was chosen and the success criteria for this test is whether Basilisk gives the same results as this BOE calculation within a certain tolerance. The spacecraft has a constant force applied through the whole simulation with the hinged rigid bodies initially undeflected and they have damping. The force is always applied through the center of mass of the spacecraft and results in no rotation of the spacecraft.

4.5 Frequency and Amplitude Verification Scenario

4.5.1 Frequency Test Description

The BOE calculation for the frequency of oscillation of flexing hinged rigid bodies when a constant force is being applied to the spacecraft is done by making simplifications to the flexing equation seen in the Model Description Section. The following assumptions are made to simplify the equations:

1. The force is being directed through the center of mass of the spacecraft, along the $\hat{\mathbf{b}}_2$ direction
2. The panels are initially undeflected and they are symmetric therefore the body will not rotate
3. Rotation is no longer apart of the equations so the translation and solar panel equations are the only equations needed
4. $\hat{\mathbf{s}}_{i,3}$ is assumed to be equal to $\hat{\mathbf{h}}_{i,3}$ in the equations of motion



At steady state, we know that
 $\sum \tau_H = 0$ because $\ddot{\theta} = 0$. Therefore,

$$\sum \tau_{com} = -k\theta_{ss} - m_{sp} a_{sp} (d \cos \theta_{ss}) = I \ddot{\theta}$$

$$a_{sp} = \frac{F}{m_{sc}}$$

$$-k\theta_{ss} = m_{sp} \left(\frac{F}{m_{sc}} \right) d \cos \theta_{ss}$$

$$f(\theta) = k\theta_{ss} + m_{sp} a_{sp} (d \cos \theta_{ss})$$

Fig. 2: Steady State Deflection BOE Calculation

5. No external torque is being applied directly to the hinged rigid bodies
6. Non-linear terms are neglected

Using the third assumption from above, the rotational motion is taken out of the equations of motion:

$$m_{sc}\ddot{\mathbf{r}}_{B/N} + \sum_i^N m_{sp_i} d_i \hat{\mathbf{s}}_{i,3} \ddot{\theta}_i = \mathbf{F}_{ext} - \sum_i^N m_{sp_i} d_i \dot{\theta}_i^2 \hat{\mathbf{s}}_{i,1} \quad (19)$$

$$m_{sp_i} d_i \hat{\mathbf{s}}_{i,3}^T \ddot{\mathbf{r}}_{B/N} + (I_{s_{i,2}} + m_{sp_i} d_i^2) \ddot{\theta}_i = -k_i \theta_i - c_i \dot{\theta}_i + \hat{\mathbf{s}}_{i,2}^T \boldsymbol{\tau}_{ext,H_i} \quad (20)$$

Next, assumptions 4-6 are applied:

$$m_{sc}\ddot{\mathbf{r}}_{B/N} + \sum_i^N m_{sp_i} d_i \hat{\mathbf{h}}_{i,3} \ddot{\theta}_i = \mathbf{F}_{ext} \quad (21)$$

$$m_{sp_i} d_i \hat{\mathbf{h}}_{i,3}^T \ddot{\mathbf{r}}_{B/N} + (I_{s_{i,2}} + m_{sp_i} d_i^2) \ddot{\theta}_i = -k_i \theta_i - c_i \dot{\theta}_i \quad (22)$$

Finally, knowing that the force is being directed along the $\hat{\mathbf{b}}_2$ axis and that the spacecraft will not rotate, the equations simplify to:

$$m_{sc}\ddot{y}_{B/N} + \sum_i^N m_{sp_i} d_i \ddot{\theta}_i = F_y \quad (23)$$

$$m_{sp_i} d_i \ddot{y}_{B/N} + (I_{s_{i,2}} + m_{sp_i} d_i^2) \ddot{\theta}_i = -k_i \theta_i - c_i \dot{\theta}_i \quad (24)$$

Converting these equations to state space:

$$\begin{bmatrix} 1 & 0 & 0 & 0 & 0 & 0 \\ 0 & m_{sc} & 0 & m_{sp_1} d_1 & 0 & m_{sp_2} d_2 \\ 0 & 0 & 1 & 0 & 0 & 0 \\ 0 & m_{sp_1} d_1 & 0 & I_{s_{1,2}} + m_{sp_1} d_1^2 & 0 & 0 \\ 0 & 0 & 0 & 0 & 1 & 0 \\ 0 & m_{sp_2} d_2 & 0 & 0 & 0 & I_{s_{2,2}} + m_{sp_2} d_2^2 \end{bmatrix} \begin{bmatrix} \dot{y}_{B/N} \\ \ddot{y}_{B/N} \\ \theta_1 \\ \dot{\theta}_1 \\ \theta_2 \\ \dot{\theta}_2 \end{bmatrix} = \begin{bmatrix} 0 & 1 & 0 & 0 & 0 & 0 \\ 0 & 0 & 0 & 0 & 0 & 0 \\ 0 & 0 & 0 & 1 & 0 & 0 \\ 0 & 0 & -k_1 & -c_1 & 0 & 0 \\ 0 & 0 & 0 & 0 & 0 & 1 \\ 0 & 0 & 0 & 0 & -k_2 & -c_2 \end{bmatrix} \begin{bmatrix} y_{B/N} \\ \dot{y}_{B/N} \\ \theta_1 \\ \dot{\theta}_1 \\ \theta_2 \\ \dot{\theta}_2 \end{bmatrix} + \begin{bmatrix} 0 \\ F_y \\ 0 \\ 0 \\ 0 \\ 0 \end{bmatrix} \quad (25)$$

Written in a more compact form:

$$[M]\dot{\mathbf{X}} = [A]\mathbf{X} + \mathbf{F} \quad (26)$$

The equivalent dynamics matrix for this coupled system is:

$$[\tilde{A}] = [M][A] \quad (27)$$

Finding the eigenvalues of $[\tilde{A}]$ will describe the coupled natural frequencies of the combined system. The integrated test for this scenario ensures that the analytical coupled frequency of oscillation matches the frequency obtained from the simulation.

4.5.2 Max Deflection While Force is Being Applied

The next BOE calculation that is needed is to find the maximum deflection while the force is being applied and when the force is not being applied (with the assumption that there is no damping). When the force is being applied the following max deflection can be seen in the following equation:

$$\theta_{\max} = 2\theta_{SS} \quad (28)$$

which uses the definition of θ_{SS} from Fig. 2.

4.5.3 Max Deflection While Force is Not Being Applied

Finally, the maximum deflection when the force is not being applied uses energy techniques. Once the force is no longer being applied, energy is conserved and the velocity of the center of mass is constant. The energy when the force is turned off is represented in the following equation:

$$E_0 = \frac{1}{2}m_{\text{hub}}\dot{y}_{B/N}^2 + 2\left[\frac{1}{2}m_{\text{sp}}\dot{\mathbf{r}}_{\text{sp}} \cdot \dot{\mathbf{r}}_{\text{sp}} + \frac{1}{2}I_{\text{sp}}\dot{\theta}^2 + \frac{1}{2}k\theta^2\right] \quad (29)$$

Where $\dot{\mathbf{r}}_{\text{sp}}$ is

$$\dot{\mathbf{r}}_{\text{sp}} = \begin{bmatrix} -d\dot{\theta} \sin(\theta) \\ \dot{y}_{B/N} + d\dot{\theta} \cos(\theta) \end{bmatrix} \quad (30)$$

Next, the velocity of the center of mass of the system is defined in the following equation:

$$v_{\text{CoM}} = \frac{1}{m_{\text{tot}}}(m_{\text{hub}}\dot{y}_{B/N} + 2m_{\text{sp}}\dot{r}_{\text{sp},y}) \quad (31)$$

This value can be computed from the values at the time the force is shut off and is a conserved quantity.

When the panels are deflected at max deflection, $\dot{\theta} = 0$. Leveraging this assumption the final energy is defined as follows:

$$E_F = \frac{1}{2}m_{\text{tot}}v_{\text{CoM}}^2 + 2\left[\frac{1}{2}k\theta_{\max}^2\right] \quad (32)$$

Conservation of energy states

$$E_0 = \frac{1}{2}m_{\text{tot}}v_{\text{CoM}}^2 + k\theta_{\max}^2 \quad (33)$$

Therefore, θ_{\max} is found using the following equation:

$$\theta_{\max} = \sqrt{\frac{E_0 - \frac{1}{2}m_{\text{tot}}v_{\text{CoM}}^2}{k}} \quad (34)$$

4.6 Lagrangian vs Basilisk Scenario

In this scenario the equations of motion for a planar simulation of a spacecraft hub and two hinged rigid bodies using Lagrangian mechanics was developed using Mathematica. The mathematica script can be seen in the support folder in the following file name: PlanarFlexibleDynamicsDerivation. This simulation is ran independently in the integrated test and the results are compared vs Basilisk results. A force and torque is applied for a certain amount of time, then turned off. Then another pulse of a force and torque is applied and turn off and the simulation runs for another few seconds.

5 Test Parameters

Since this is an integrated test, the inputs to the test are the physical parameters of the spacecraft along with the initial conditions of the states. These parameters are outlined in Tables 2- 5. Additionally, the error tolerances can be seen in Table 6.

Table 2: Spacecraft Hub Parameters

Name	Description	Value	Units
mHub	mass	750.0	kg
IHubPntBc_B	Inertia in \mathcal{B} frame	$\begin{bmatrix} 900.0 & 0.0 & 0.0 \\ 0.0 & 600.0 & 0.0 \\ 0.0 & 0.0 & 600.0 \end{bmatrix}$	kg-m ²
r_BcB_B	CoM Location in \mathcal{B} frame	$[0.0 \ 0.0 \ 1.0]^T$	m

Table 3: Hinged Rigid Body 1 Parameters

Name	Description	Value	Units
mass	mass	100.0	kg
IPntS_S	Inertia in \mathcal{S} frame	$\begin{bmatrix} 100.0 & 0.0 & 0.0 \\ 0.0 & 50.0 & 0.0 \\ 0.0 & 0.0 & 50.0 \end{bmatrix}$	kg-m ²
d	CoM location	1.5	m
k	Spring Constant	100.0	N-m/rad
c	Damping Term	0.0 (6.0 - damping scenario)	N-m-s/rad
r_HB_B	Hinge Location in \mathcal{B} frame	$[0.5 \ 0.0 \ 1.0]^T$	m
dcm_HB	\mathcal{B} to \mathcal{H} DCM	$\begin{bmatrix} -1.0 & 0.0 & 0.0 \\ 0.0 & -1.0 & 0.0 \\ 0.0 & 0.0 & 1.0 \end{bmatrix}$	-

Table 4: Hinged Rigid Body 2 Parameters

Name	Description	Value	Units
mass	mass	100.0	kg
IPntS_S	Inertia in \mathcal{S} frame	$\begin{bmatrix} 100.0 & 0.0 & 0.0 \\ 0.0 & 50.0 & 0.0 \\ 0.0 & 0.0 & 50.0 \end{bmatrix}$	kg-m ²
d	CoM location	1.5	m
k	Spring Constant	100.0	N-m/rad
c	Damping Term	0.0 (7.0 - damping scenario)	N-m-s/rad
r_HB_B	Hinge Location in \mathcal{B} frame	$[-0.5 \ 0.0 \ 1.0]^T$	m
dcm_HB	\mathcal{B} to \mathcal{H} DCM	$\begin{bmatrix} 1.0 & 0.0 & 0.0 \\ 0.0 & 1.0 & 0.0 \\ 0.0 & 0.0 & 1.0 \end{bmatrix}$	-

Table 5: Initial Conditions for Energy Momentum Conservation Scenarios

Name	Description	Value	Units
(Panel 1) thetaInit	(Panel 1) Initial θ	5.0	deg
(Panel 1) thetaDotInit	(Panel 1) Initial $\dot{\theta}$	0.0	deg
(Panel 2) thetaInit	(Panel 2) Initial θ	0.0	deg
(Panel 2) thetaDotInit	(Panel 2) Initial $\dot{\theta}$	0.0	deg
r_CN_NInit	Initial Position of S/C (gravity scenarios)	$[-4020339 \ 7490567 \ 5248299]^T$	m
v_CN_NInit	Initial Velocity of S/C (gravity scenarios)	$[-5199.78 \ -3436.68 \ 1041.58]^T$	m/s
r_CN_NInit	Initial Position of S/C (no gravity)	$[0.1 \ -0.4 \ 0.3]^T$	m
v_CN_NInit	Initial Velocity of S/C (no gravity)	$[-0.2 \ 0.5 \ 0.1]^T$	m/s
sigma_BNInit	Initial MRP of \mathcal{B} frame	$[0.0 \ 0.0 \ 0.0]^T$	-
omega_BN_BInit	Initial Angular Velocity of \mathcal{B} frame	$[0.1 \ -0.1 \ 0.1]^T$	rad/s

Table 6: Error Tolerance - Note: Relative Tolerance is $\text{abs}(\frac{\text{truth}-\text{value}}{\text{truth}})$

Test	Relative Tolerance
Energy and Momentum Conservation	1e-10
Steady State Deflection	1e-6
Frequency verification	5e-3
Max deflection with force on	5e-3
Max deflection with force off	5e-3
Lagrangian vs Basilisk comparison	1e-10

6 Test Results

The following figures show the conservation of the quantities described in the success criteria for each scenario. The conservation plots are all relative difference plots. All conservation plots show integration error which is the desired result. In the python test these values are automatically checked therefore when the tests pass, these values have all been confirmed to be conserved.

6.1 Gravity with no damping scenario

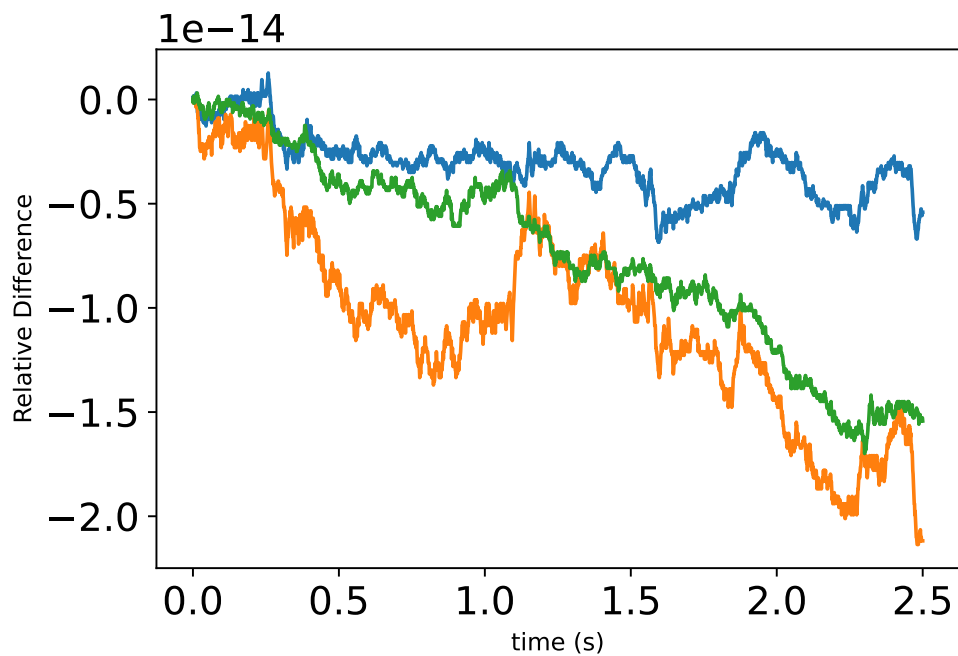


Fig. 3: Change in Orbital Angular Momentum with Gravity

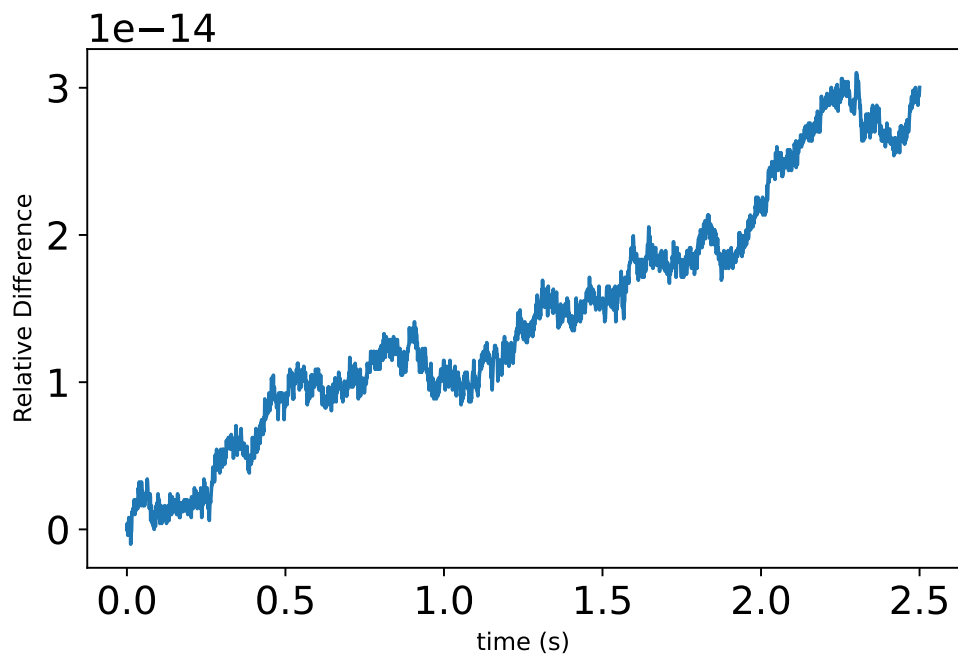


Fig. 4: Change in Orbital Energy with Gravity

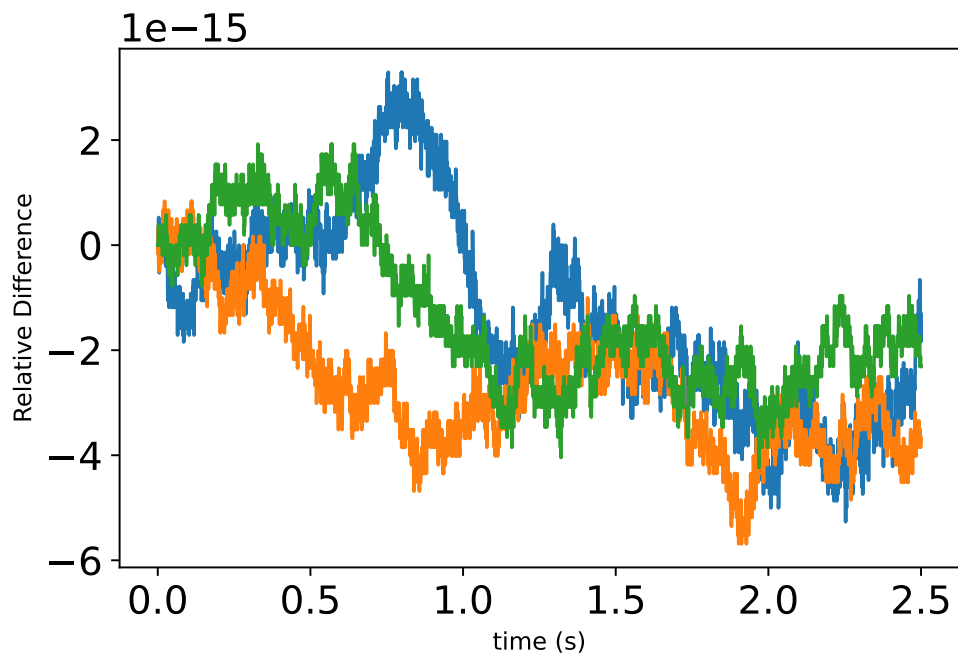


Fig. 5: Change In Rotational Angular Momentum with Gravity

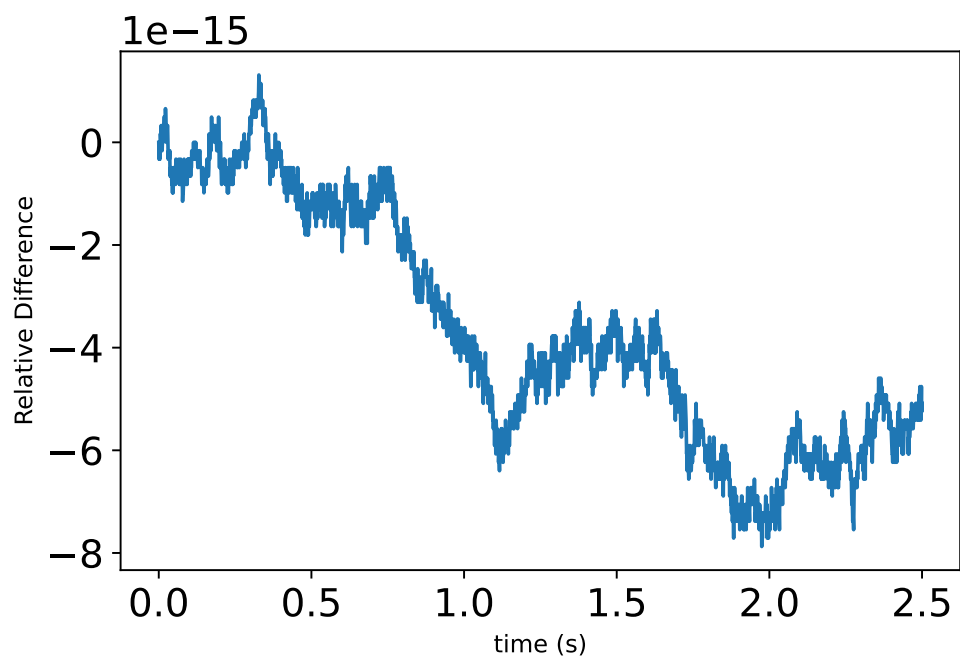


Fig. 6: Change In Rotational Energy with Gravity

6.2 No Gravity with no damping scenario

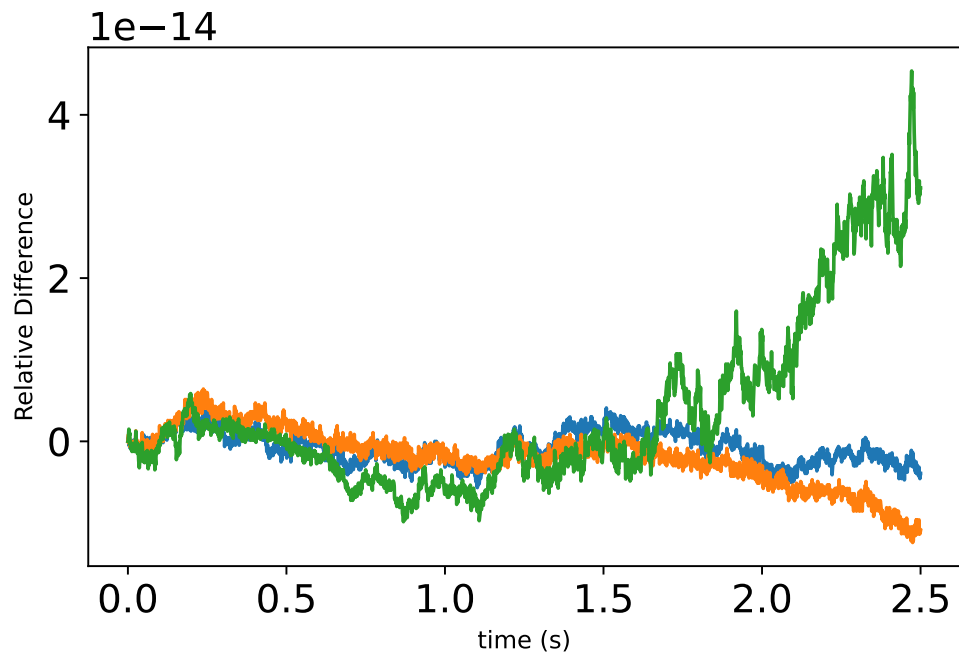


Fig. 7: Change in Orbital Angular Momentum No Gravity

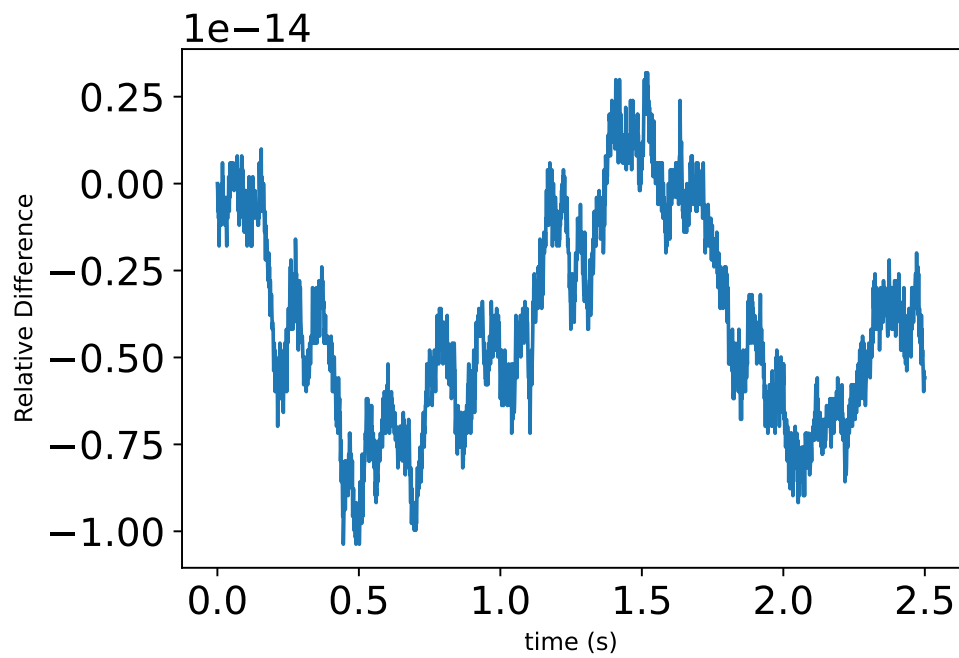


Fig. 8: Change in Orbital Energy No Gravity

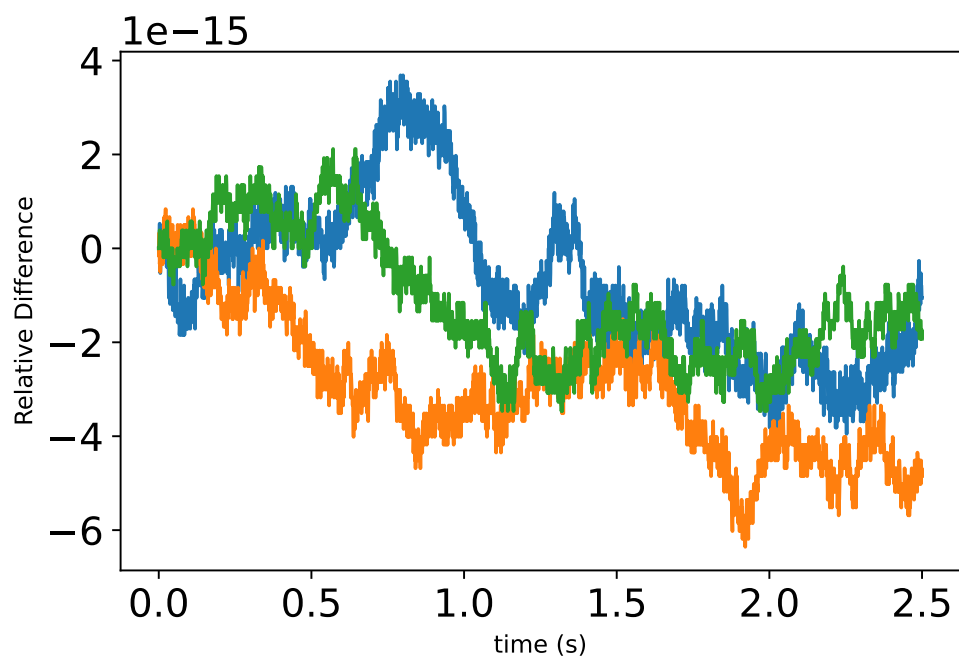


Fig. 9: Change In Rotational Angular Momentum No Gravity

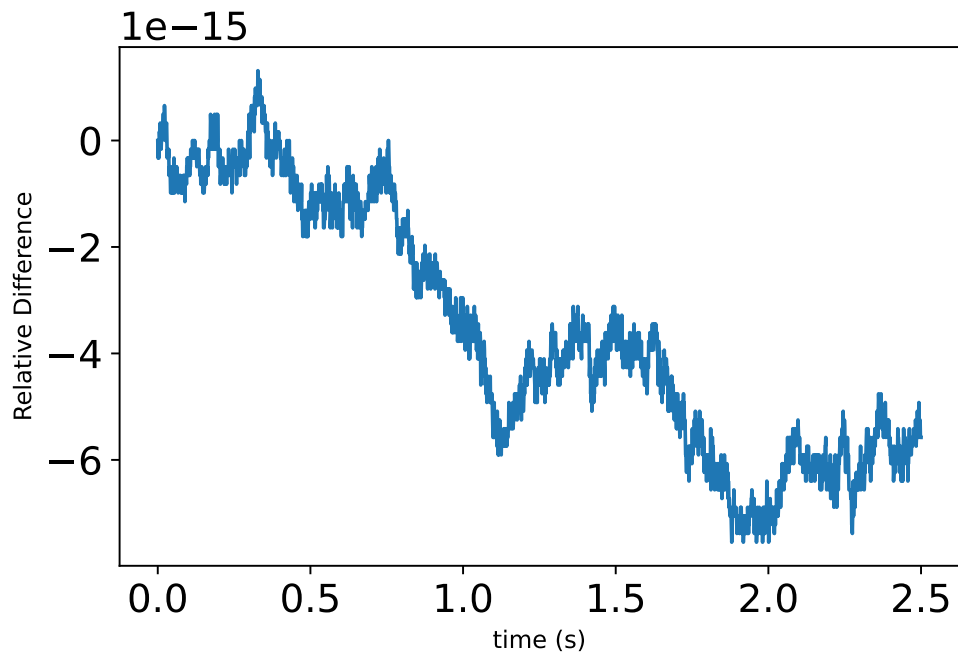


Fig. 10: Change In Rotational Energy No Gravity

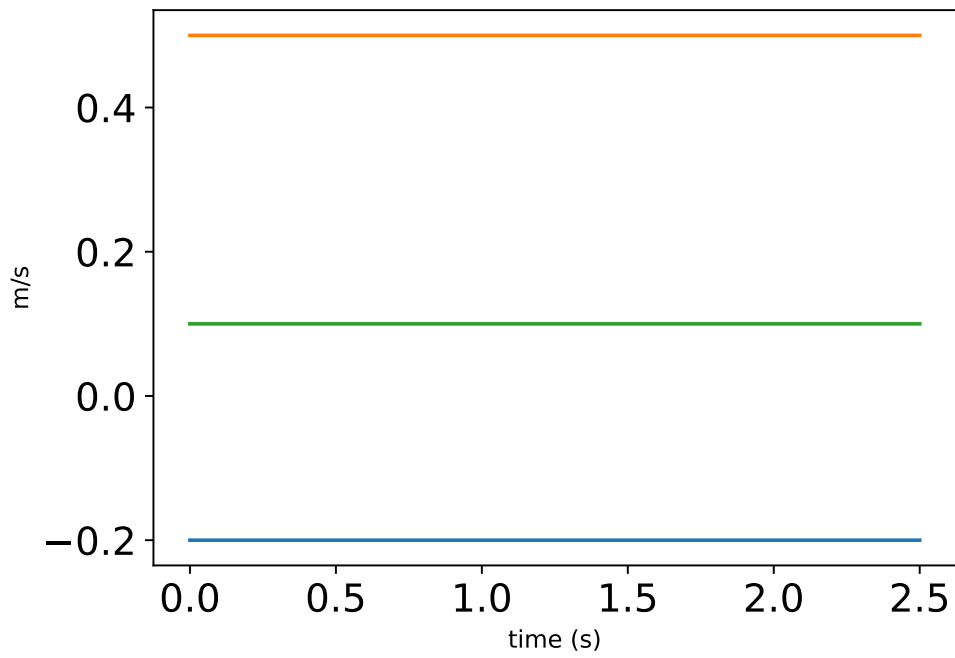


Fig. 11: Velocity Of Center Of Mass No Gravity

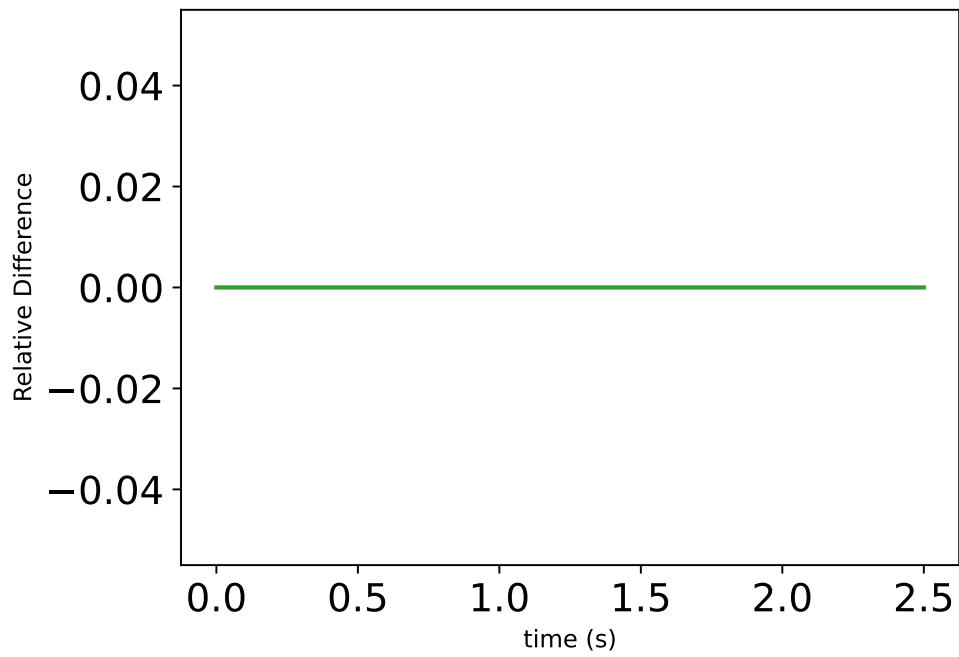


Fig. 12: Change In Velocity Of Center Of Mass No Gravity

6.3 No Gravity with damping scenario

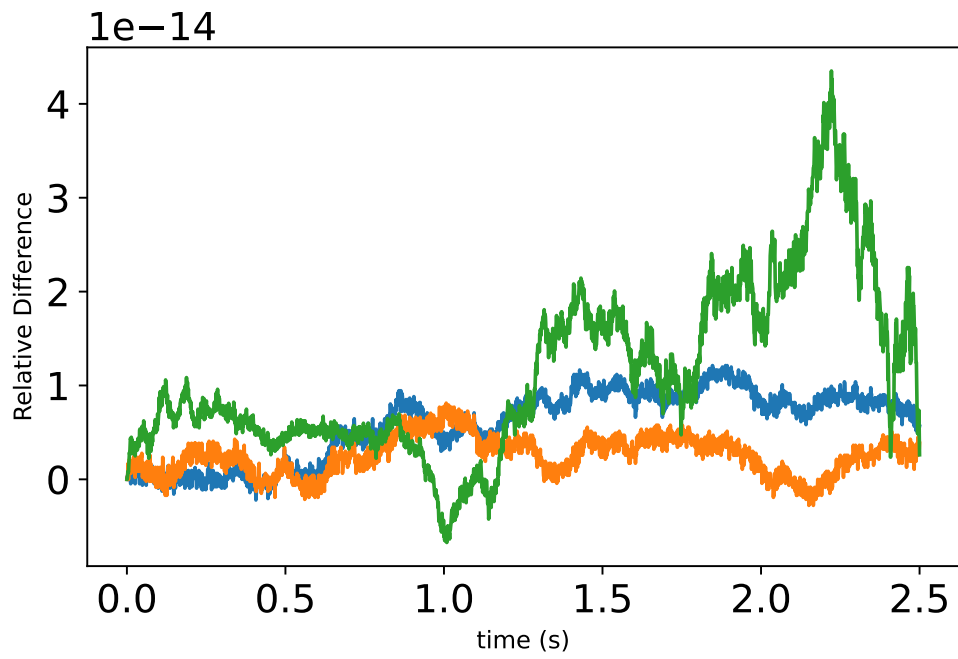


Fig. 13: Change in Orbital Angular Momentum No Gravity with Damping

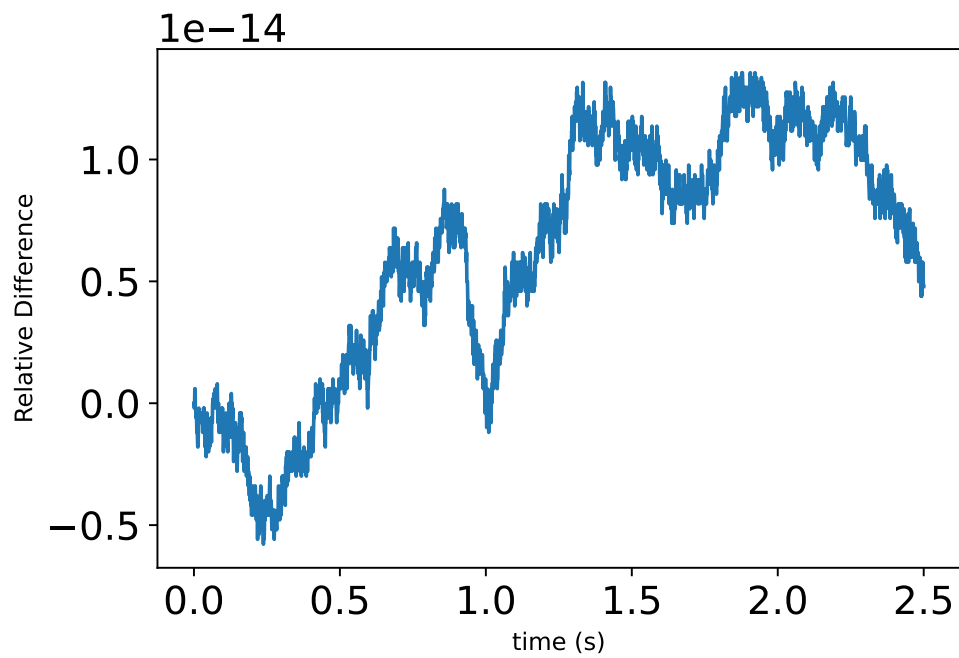


Fig. 14: Change in Orbital Energy No Gravity with Damping

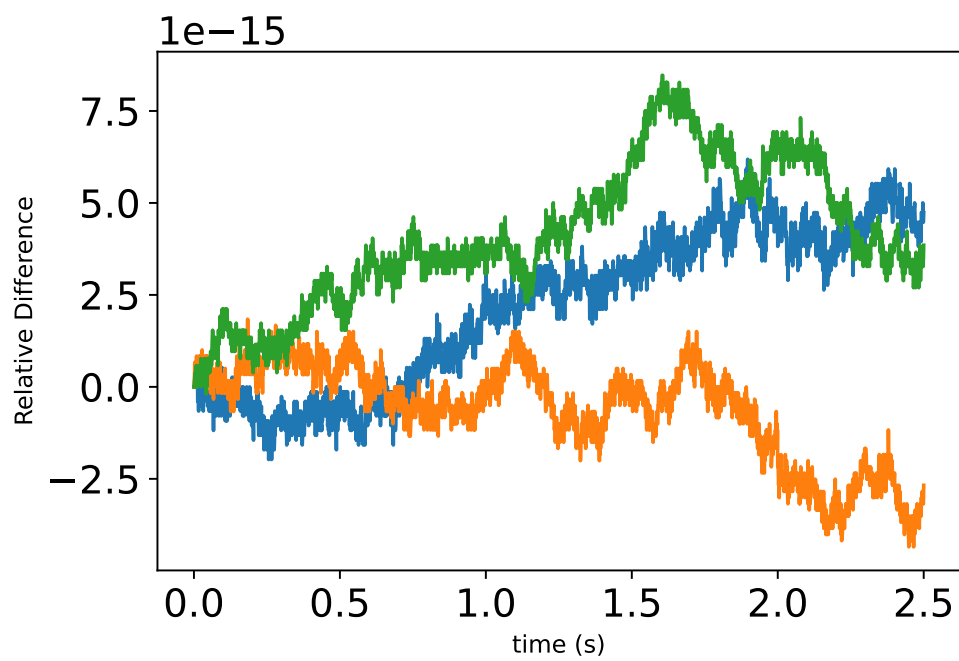


Fig. 15: Change In Rotational Angular Momentum No Gravity with Damping

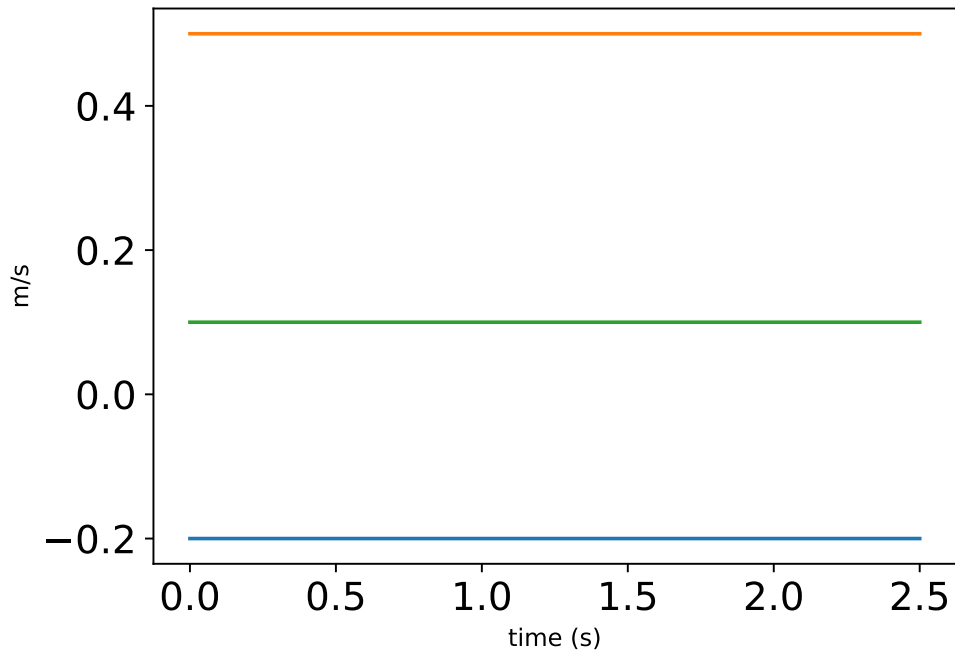


Fig. 16: Velocity Of Center Of Mass No Gravity with Damping

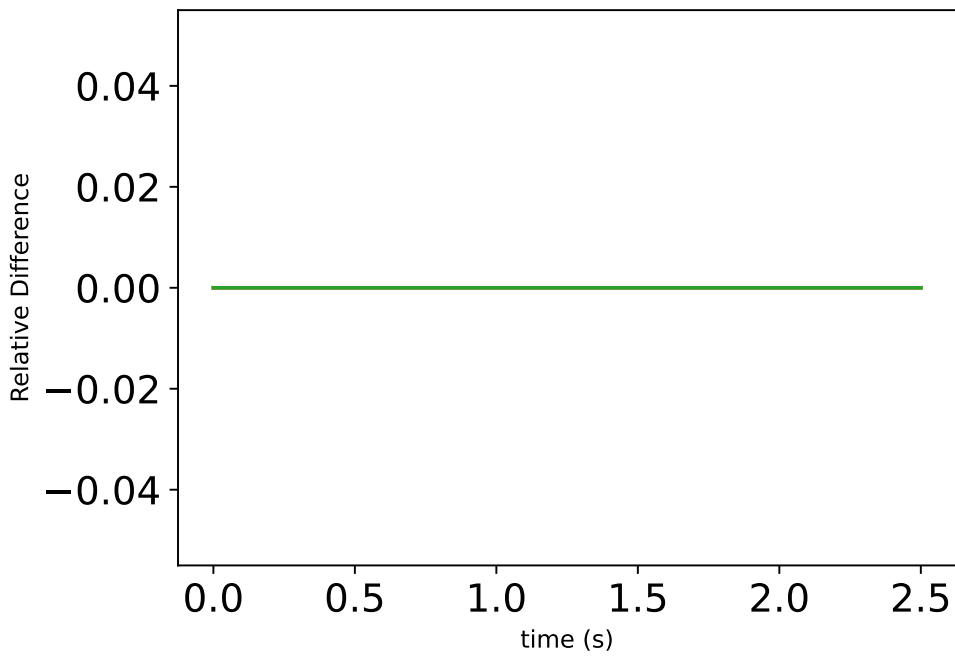


Fig. 17: Change In Velocity Of Center Of Mass No Gravity with Damping

6.4 Steady State Deflection Scenario

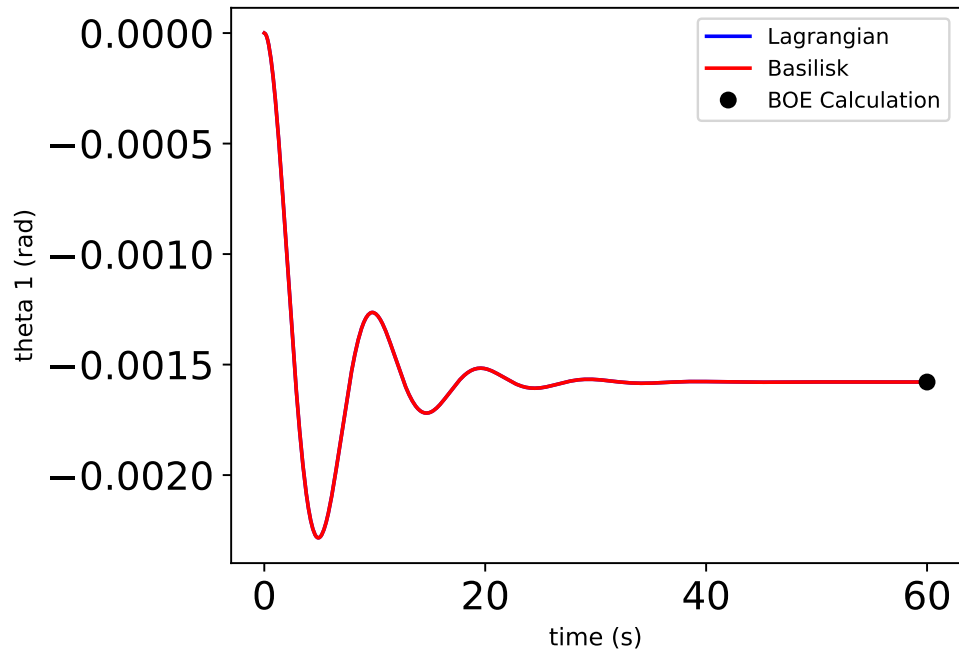


Fig. 18: BOE Calculation for Steady State Theta 1 Deflection vs Simulation

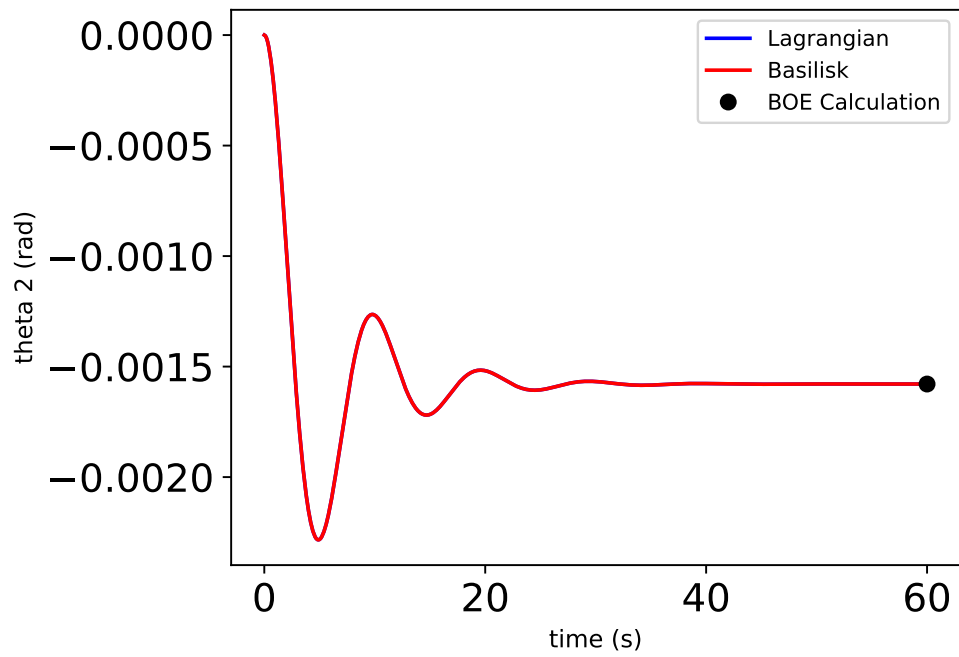


Fig. 19: BOE Calculation for Steady State Theta 2 Deflection vs Simulation

6.5 Frequency and Amplitude Verification Scenario

Table 7: Frequency and Amplitude Test Results

Name	BOE Calculation	Basilisk Results	Relative Error
Frequency	0.18271091965072633	0.18348623853211005	0.004243418416730797
Theta Max 1	-0.0010526314331535647	-0.0010525980610644567	3.170348904364788e-05
Theta Max 2	0.0008488839273411005	0.0008488531651652984	3.623837701635495e-05

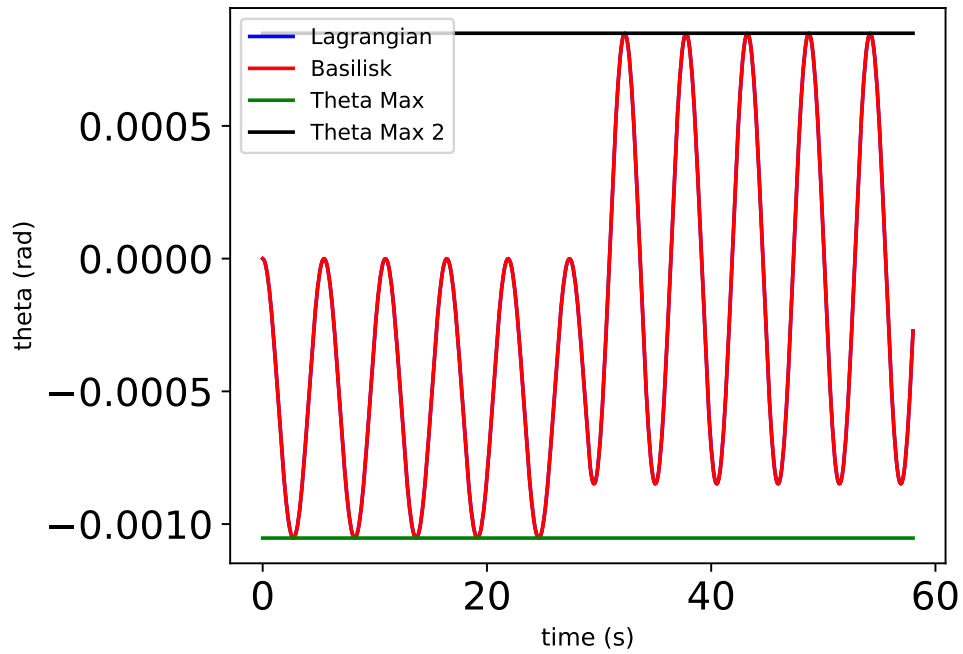


Fig. 20: Max Theta While Forcing

6.6 Lagrangian vs Basilisk Scenario

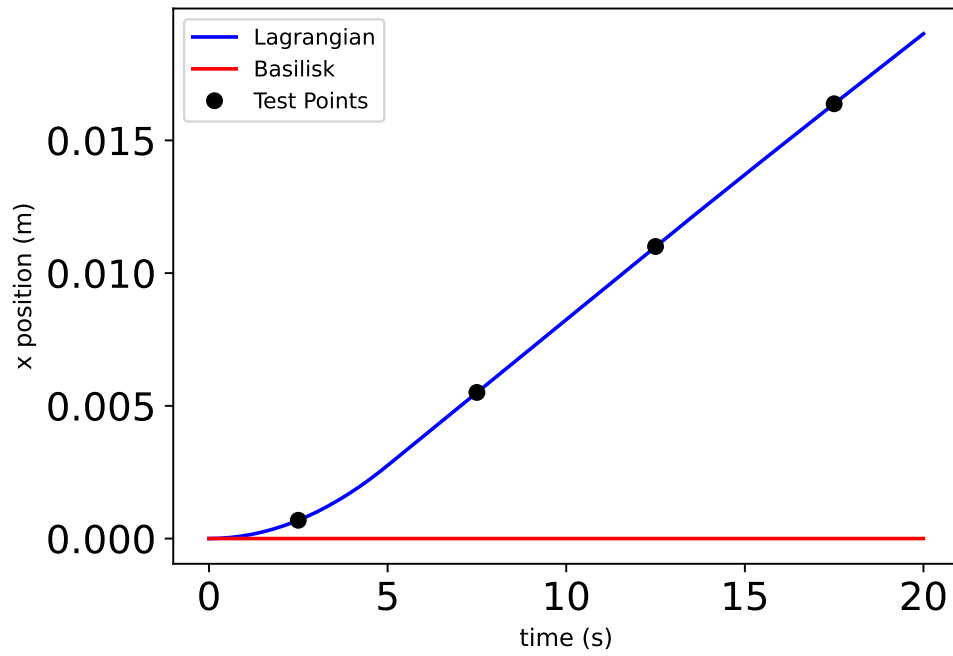


Fig. 21: X Position Lagrangian Vs Basilisk

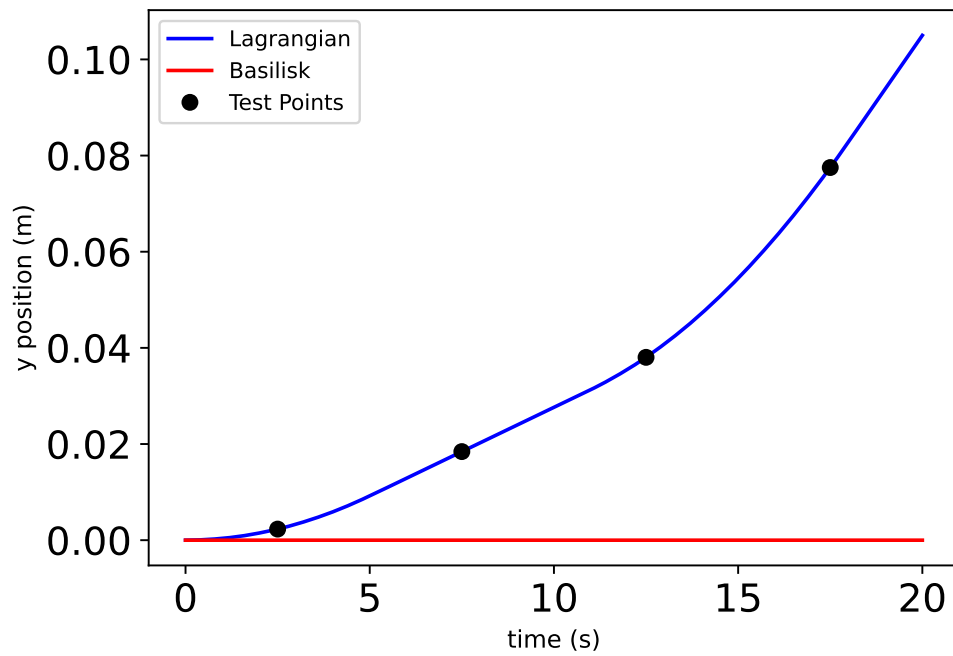


Fig. 22: Y Position Lagrangian Vs Basilisk

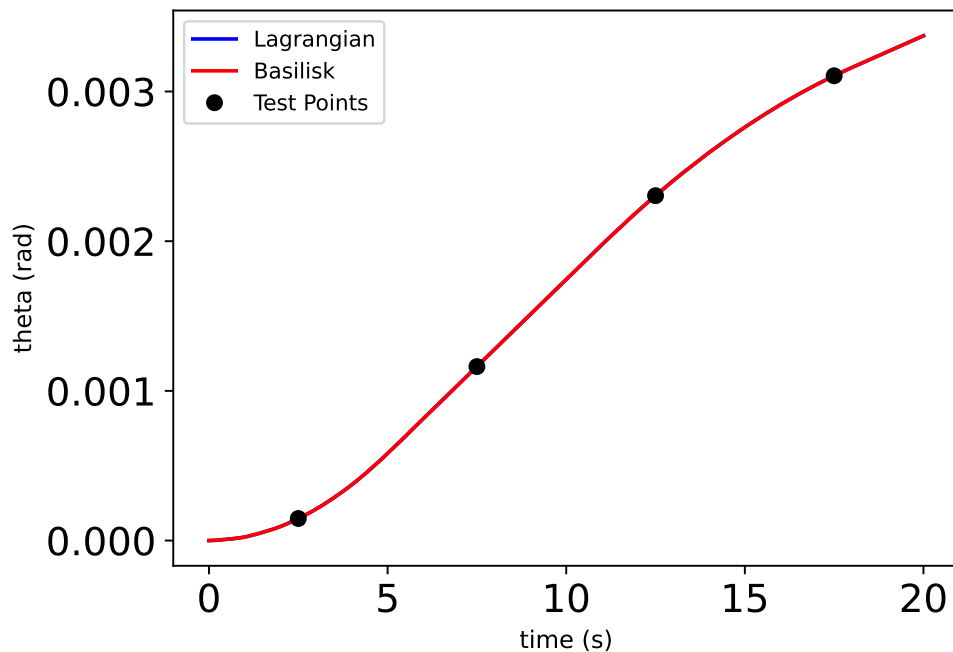


Fig. 23: Theta Lagrangian Vs Basilisk

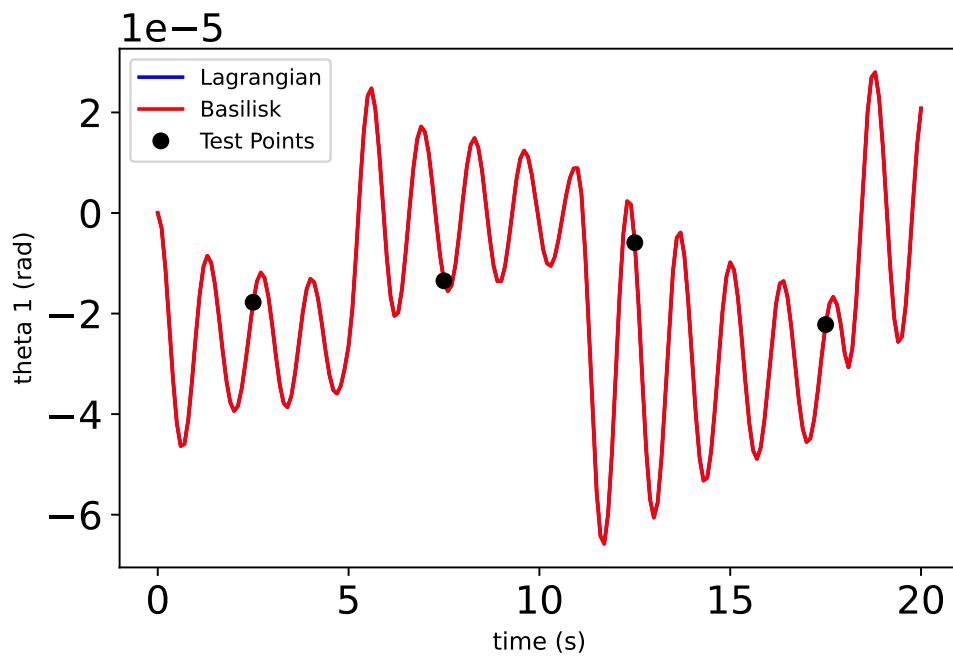


Fig. 24: Theta 1 Position Lagrangian Vs Basilisk

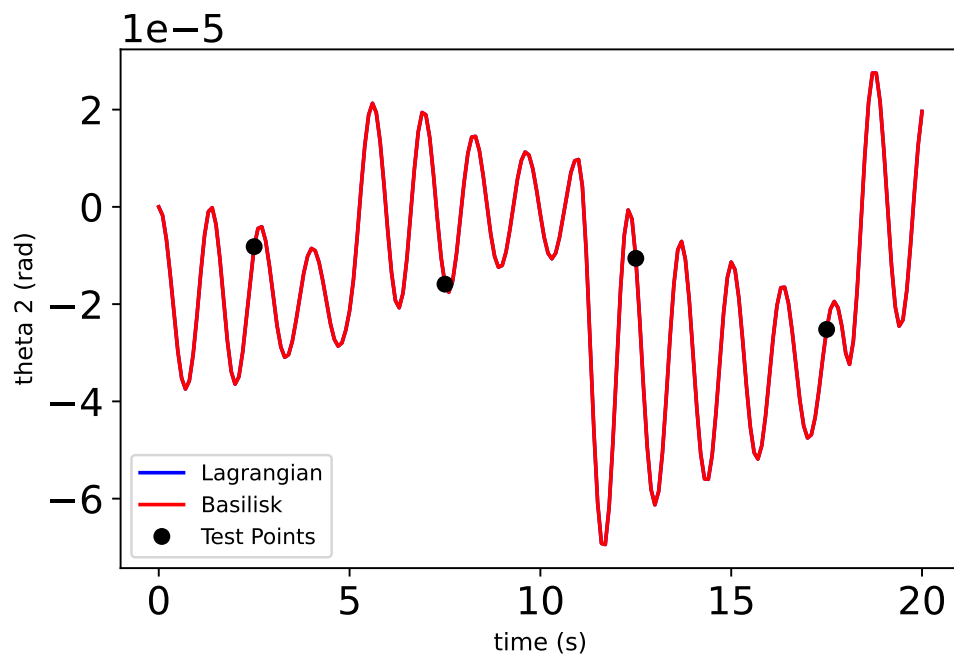


Fig. 25: Theta 2 Lagrangian Vs Basilisk

REFERENCES

- [1] C. Allard, Hanspeter Schaub, and Scott Piggott. General hinged solar panel dynamics approximating first-order spacecraft flexing. In *AAS Guidance and Control Conference*, Breckenridge, CO, Feb. 5–10 2016. Paper No. AAS-16-156.